https://doi.org/10.65542/djei.v2i1.30
*Dasinya Journal for Engineering and Informatics*. 2026, 2, 5.

*Review*

# Harnessing Natural Dyes and Nanomaterials for DSSC Innovation: A Review of Experimental and Materials Trends

**Ivan H. Hameed [1], Maher K. Ali [2], Shinwar A. Idrees [3,*]**

[1] Department of Environment, College of Science, University of Zakho, Kurdistan Region, Iraq
[2] Department of Chemistry, College of Science, University of Zakho, Kurdistan Region, Iraq
[3] Research Center, University of Zakho, Kurdistan Region, Iraq
[*] Correspondence: shinwar.idrees@uoz.edu.krd

**Abstract**

This review covers recent developments in dye-sensitized solar cells, focusing on natural pigments, nanostructures in photoanodes, and modifications to electrolytes, which all relate to the enhancement of device performance. Anthocyanins, chlorophyll, and carotenoids are some natural dyes that are under investigation as alternatives to ruthenium-based synthetic dyes. However, they still have some drawbacks due to their restricted absorption spectra and low stability. Enhanced extraction methods have realized 30% gains in dye performance. The design and composition of the photoanode play a significant role in DSSC efficiency. The latest progress in doping $TiO_2$ with materials like silver and graphene, adding other semiconductors such as ZnO and $MoS_2$, has established efficiencies as high as 10.35% for DSSCs. Moreover, interface modification, especially the use of alternative electrolytes, replacing the conventional iodide/triiodide system with cobalt, copper complexes, has attained higher efficiencies up to 14.4%. However, stability in volatile solvents remains a challenge. This review considers DSSCs to become one of the practical renewable energy technologies, yet some important limitations, together with ways for future research, are emphasized.

**Keywords:** DSSCs; Natural dyes; Photoanodes; Nanoparticles; Electrolyte solution.

## 1. Introduction

The pioneering work by Michael Grätzel and Brian O'Regan on the use of nanoscale porous $TiO_2$ film electrodes in dye-sensitized solar cells marked the start of the development of sensitized solar cells. Dye dye-sensitized solar cell operates through the conversion of sunlight to usable electricity by the photoelectric effect [1] [2]. These cells use the photoelectric effect, acting as energy converters that change sunlight into electrical power [1] [2]. These cells have gained a lot of attention due to their simple fabrication process and are low in cost with minimum environmental impact compared to silicon-based photovoltaic technologies. However, the pervasive use of ruthenium in dye components creates significant challenges in increasing the overall production cost of this technology. In view of this consideration, it is an urgent need to explore other alternative dye materials that are both more efficient and economically viable [3].

While the efficiency achieved so far by DSSC is about 13%, it holds great promise for clean, renewable energy applications [4]. Commercial dyes containing heavy transition metals, especially ruthenium-based molecules, usually yield 11–12% power conversion efficiencies using nano-porous titania electrodes [5, 6]. However, ruthenium complexes contain ecologically harmful heavy metals [7]. Their high costs and limited availability [8] drive the search for alternative photosensitizers. Natural dyes offer similar efficiency.

Received: November 8, 2025; Revised: December 26, 2025; Accepted: January 7, 2026; Published: January 25, 2026; Available online: January 25, 2026.
**Copyright:** © 2026 by the authors. Submitted for possible open access publication under the terms and conditions of the Creative Commons Attribution (CC BY) license (https://creativecommons.org/licenses/by/4.0/).

Furthermore, Natural dye pigments can be found in various plant parts, including the flowers, fruits, leaves, stems, and roots, positioning them as a promising option for DSSC photosensitizers. Nonetheless, several significant challenges must be overcome before they can be commercially utilized at a large scale. Key issues regarding dye conservation include rapid degradation, instability, and a brief shelf life. Although these coloring compounds exist, they exhibit a more restricted absorption spectrum, which diminishes photon capture efficiency. Notably, flavonoids and anthocyanins are among the most important natural dyes, commonly present in fruits and flowers [9].

These dyes efficiently absorb radiation within the visible region of the spectrum, precisely in the region of 520 to 560 nm 10. The adsorption of anthocyanin onto the surface of $TiO_2$ can occur mainly because of Van der Waals attraction, since this happens due to bonding between two oxygen atoms of anthocyanin with the $Ti^{4+}$ ion at the surface of $TiO_2$- where two of the bonding sites are unoccupied and positively charged [11]. In light of these points, a review encompasses recent advances in developing natural dye-sensitized solar cells. It discusses DSSC processes, natural dyes, material characterizations, efficiency, and strategies for improving device performance.

The most widely used semiconductor for the photoanodes of DSSC is titanium dioxide ($TiO_2$), due to its high surface area, stability, and suitable energy band alignment. Having said that, porosity of the $TiO_2$ film is important for light absorption and transport of electrons; it is achievable with modifications in doping and at the surface, as noted by O'Regan and Grätzel (1991) [12] [13]. Other metal oxides, such as ZnO and CuO, have also been explored as potential photoanode materials. However, their practical applications are significantly limited because ZnO degrades quickly in acidic conditions, and CuO has very poor conduction band alignment, making the DSSCs less durable and less efficient. Consequently, titanium dioxide is still the most common choice in most DSSC applications [14] [15].

Moreover, it optimizes different parameters like dye, photoanode material, electrolyte, and device structure for DSSC efficiency. Recently, it was reported that the doping of $TiO_2$ with nanoparticles of silver or graphene would enhance charge transfer and reduce recombination. For example, Ghosh et al. (2021) reported that when nano-silver-doped graphene was incorporated into $TiO_2$, it improved the efficiency of the cell up to 9.9%, which was quite remarkable compared with undoped ones, giving emphasis on the nanostructure modification in cells [16].

Moreover, natural dyes are responsible for the determination of the efficiency and stability of DSSCs. Natural pigments such as flavonoids, chlorophyll, and carotenoids are potential alternatives to synthetic dyes. Flavonoids, in particular anthocyanins, are widely found in flowers and fruits and show strong light-harvesting characteristics in the visible spectrum and hence are good sensitizers. Carotenoids, i.e., β-carotene, absorb light between 550 nm and are responsible for blue-green light harvesting, but are less efficient. Chlorophylls, specifically chlorophyll a, are valuable photosynthetic pigments with good absorption but poorer stability under DSSC conditions.

Carotenoids such as β-carotene have absorption at 550 nm and provide light harvesting in the blue-green region, but with less efficiency. Chlorophylls, especially chlorophyll a, are important photosynthetic pigments that have promising absorption but lower stability under conditions of DSSC. Besides, the methods of extraction that were applied to the natural dyes contribute an essential role in the stability and efficiency determination of DSSC. Narayan et al reported improvement in the extraction conditions to enhance the stability and overall efficiency of the natural solar cell with dye. Efficiency increased by 30% [17] [18] [19].

## 2. Materials and Methods

The general structure of dye-sensitized solar cells consists of an electrolyte, a natural dye, a photoanode, and a counter electrode. In the photoanode, a nanostructured semiconductor is used-nanorods, nanotubes, nanowires, nano-cones, or nanosheets manufactured on transparent conducting glass [20]. DSSCs are solar cells that use a nanostructured semiconductor layer coated with a photosensitive organic dye to convert. This nanostructured film offers a high surface area for effective dye adsorption and light capture. Such an arrangement enables electron injection and transport for improved efficiency gain [21].

A counter electrode, semiconductor oxide material, transparent conductive oxide (TCO), dye sensitizer, and electrolyte solution form a basic dye-sensitized solar cell (DSSC). The conducting glass working electrode consists of a nano-porous semiconductor oxide and is separated from the counter electrode by a thin layer of electrolyte solution. Being attracted to its surface due to adhesive properties, the dye can be prolonged on the photovoltaic cell to absorb lower-energy photons. The dye absorbs on the semiconductor surface; the absorption of visible light and stability of the dye are essential for the generation of charges [22]. In addition to this, a thick (approximately 10 μm) $TiO_2$ layer and sometimes ZnO constitute the photo-anode of a DSSC. Instead of $TiO_2$, $SnO_2$ nanoparticles are sometimes used. The

$TiO_2$ layer possesses a large inherent surface area; hence, scattering of sunlight significantly improves. Optimizing semiconductor band gap and structure is a crucial aspect for achieving high photoelectrochemical performance [23].

In addition, cell function is quite interesting, as shown in Figure 1 represents the working principle of a DSSC, where visible light is absorbed by a dye to inject an electron into a semiconductor. The HOMO to LUMO promotion of an electron occurs in the dye molecule bound to the photoelectrode, typically made of nanostructured $TiO_2$, after absorption, because it signifies the first empty level in any molecule. The highest level in such molecules is referred to as HOMO. "For the dye molecule to be a viable photosensitizer in dye-sensitized cells, it must have very strong absorption in the visible part of sunlight [24, 25]. The objective here is to have this excited electron participate in generating numerous charge carriers by entering the wide conduction band of the mesoporous $TiO_2$. The electron then moves to the transparent conductive oxide layer and eventually to the counter electrode via an external circuit.

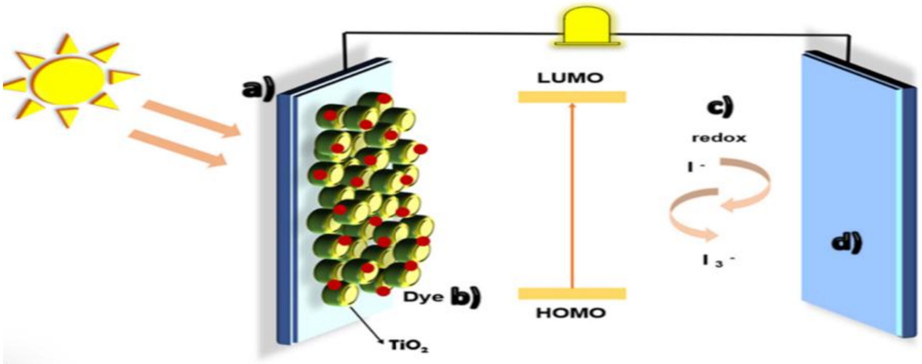


**Figure 1. The basic configuration of a DSSC consists of four major components. These are labeled below as (a), (b), (c), and (d). (a) Photo-anode. It consists of a semiconductor oxide layered on a transparent surface. (b) Photosensitized dye. These are dye materials bonded to the semiconductor coating in (a). (c) Electrolyte. It contains a redox pair. (d) Counter electrode. In this component, carbon graphite and platinum thin films can be used [27].**

### *2.1. DSSCs construction process*

A typical DSSC cell consists of a photoanode, counter electrode, dye layer, electrolyte layer, and substrate. Figure 1. shows the components of a conventional DSSC cell. The photoanode is generally a mesoporous TiO2 layer with a thickness of about 10 microns and a particle size of about 20 nanometers deposited on an FTO-coated glass substrate.

The mesoporous layer enables a high surface area where the dyes can be easily adsorbed. The counter electrode typically consists of a platinum or carbon layer and completes the DSSC cell by facilitating the redox reaction of the electrolyte layer [28].

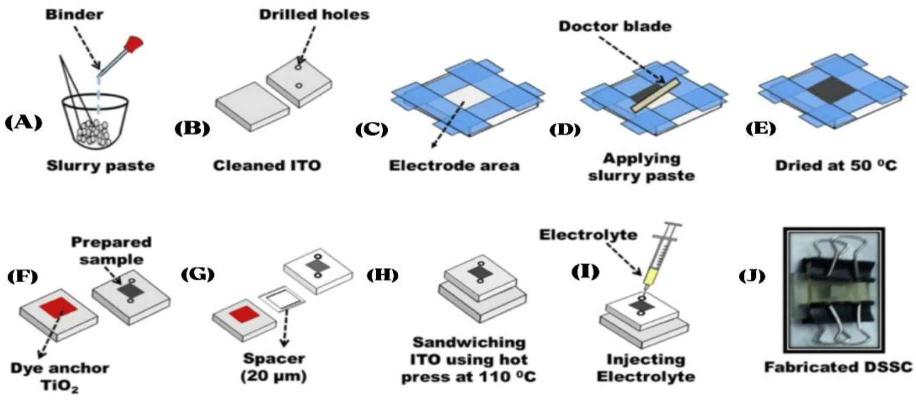


**Figure 2. Flow chart describing the procedural steps to assemble the DSSC: (a) preparation of the titanium dioxide paste including the binder, (b) cleaning and pre-drilled ITO substrate, (c) demarcation of the functional region, (d) titanium dioxide thin film formation by the doctor blade method, (e) low-temperature drying at 50 °C, (f) dye sensitization of the titanium dioxide photoanode, (g) insertion of the 20 μm spacer, (h) sealing the device at 110 °C, (i) injection of the electrolyte, and (j) assembled DSSC [30].**

## 3. Results

It has been previously demonstrated that natural dyes can serve as cost-effective and environmentally sound photosensitizers for dye-sensitized solar cells. Some of these materials have even been submitted to intensive research. They include anthocyanin pigments from fruits like blackberries and hibiscus. They have been extensively explored for their high ability to ideally absorb sunlight. According to research by Calogero et al. (2010), the efficiencies reported for natural organic dyes range from 1.5% depending on dye preparation techniques and pH values." Despite their lower efficiencies relative to synthetic materials, their ease of preparation and nontoxicity make them excellent materials to be applied for solutions related to renewable sources of energy.

The role of DSSC in bringing about sunlight into electric power makes it a very efficient and cost-effective photovoltaic device. The main success of dye-sensitized cells revolves around their sensitization from the particular dye applied to them. Natural materials act as an excellent alternative to rare materials as they cost very little and can be easily biodegradable. These sensitisers can be seen in fruits, leaves, flowers, and even plant petals. The performance of these DSSCs is given quite a boost by the characteristics of these pigments, together with some other factors. The organic dye performs very well in diffused and colourful light. They're also environmentally friendly. In the past ten years, researchers have tried to make use of different parts of plants [32].

Inorganic dyes such as ruthenium are also considered to be very essential for the development of high-efficiency DSSCs. They have high costs and difficult cleaning processes. Natural dyes have proved to be ideal substitutes for expensive and difficult-to-find inorganic materials. Nevertheless, low cost of production, ease of use, quick payback time, flexibility, availability of sources of raw materials, and non-offending risk are some advantages associated with the use of natural pigments as sensitizers [33].

Conversely, the results for fill factor (FF), power conversion efficiency (η%), open-circuit voltage (Voc), and short-circuit current (Isc) showed a comparative result to the sensitized dye. The variations in natural material dyes, such as photosensitizers in DSSC, have been shown to influence several elements in a plant cell [34].

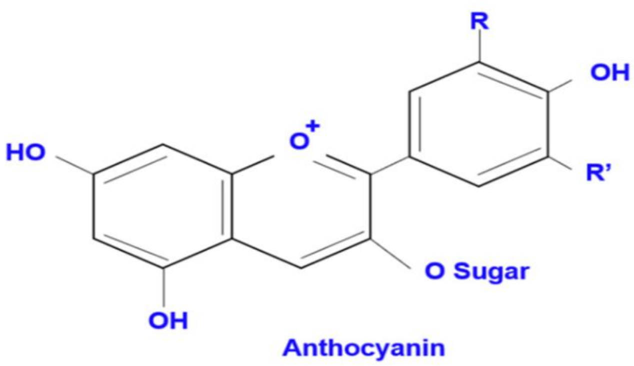


**Figure 3. Chemical structure of anthocyanin, where R stands for the glycosidic moiety. The −OH and oxygen-containing functional groups in anthocyanin are responsible for the binding of the dye molecules to the surface of TiO2 in DSSCs [3].**

However, this literature review also concentrates on natural dyes. Indeed, as they represent one of the main features in the workings of a DSSC and have been studied by several researchers, the relevant literature about this topic has been compiled in Table 1 below.

**Table 1. DSSCs' performance using dye solution measured under standard AM 1.5G illumination with an active area of 2 cm-2**

| Dye Solution | Solvent | Voc (mV) | FF (%) | η (%) | Ref. |
|---|---|---|---|---|---|
| **80% beetroot + 20% spinach** | **Ethanol** | **386 mV** | **55.0** | **0.92** | **[35]** |
| **20% malabar spinach + 80% red spinach** | **Ethanol** | **385 mV** | **51.0** | **0.84** | **[36]** |
| **Cassia fistula** | **Ethanol** | **0.51 V** | **65.0** | **0.21** | **[37]** |

| | | | | | |
|---|---|---|---|---|---|
| **Spinach leaves** | **Acetone** | **0.59 V** | **58.0** | **0.17** | **[37]** |
| **Purple cabbage** | **Oxygenated water** | **0.48 V** | **46.0** | **0.15** | **[38]** |
| **Onion** | **Oxygenated water** | **0.51 V** | **46.0** | **0.10** | **[38]** |
| **Cornelian cherry** | **Acid solvent** | **0.39 V** | **31.0** | **0.98** | **[39]** |
| **Cherry St. Lucia** | **Ethanol** | **0.56 V** | **55.0** | **0.19** | **[39]** |
| **Yellow jasmine berries** | **Ethanol** | **0.49 V** | **49.0** | **0.04** | **[40]** |
| **Madder berries** | **Ethanol** | **0.58 V** | **48.0** | **0.13** | **[40]** |
| **Crocus sativus** | **Ethanol** | **0.43 V** | **48.0** | **0.51** | **[41]** |
| **Allium Cepa** | **Ethanol** | **0.55 V** | **46.0** | **0.54** | **[42]** |
| **Malaw sylvestris** | **Ethanol** | **0.49 V** | **42.0** | **0.45** | **[43]** |
| **Malaysian Areca Catechu** | **Methanol, ethanol** | **0.539 V** | **72.0** | **0.07** | **[44]** |
| **Purple cabbage** | **Methanol, acetic acid** | **0.34 V** | **63.0** | **0.024** | **[45]** |
| **Purple cabbage** | **Acetone** | **525 mV** | **59.0** | **0.07** | **[45]** |
| **Turmeric longa L.** | **Ethanol** | **566 mV** | **29.0** | **0.029** | **[46]** |
| **Berberis vulgaris** | **Methanol** | **568 mV** | **40.0** | **0.09** | **[47]** |
| **Phytolacca americana** | **Ethanol** | **0.570 V** | **56.0** | **0.05** | **[48]** |
| **Musa acuminata** | **Ethanol, Acetic acid** | **0.58 V** | **59.0** | **0.31** | **[49]** |
| **60% turmeric + 40% red spinach** | **Ethanol** | **499 mV** | **57.0** | **1.07** | **[50]** |

Current developments in dye-sensitized cells have reminded researchers about the importance of electrolyte composition to overall efficiency. In terms of performance and durability, A 14.3% power conversion efficiency (η) was reported by Smith et al. [51] employing $[Co(phen)_3]^{3+/2+}$ complexes in acetonitrile solution with ADEKA-1 and LEG4 dye sensitizers. The results in Table 2 show the ability of the metal complex to provide high open-circuit voltage values compared to conventional iodide-based cells.

**Table 2 illustrates that the cobalt complex yields higher open-circuit voltages than conventional iodide systems under standard AM 1.5G illumination with active area of 2 cm$^{-2}$**

| Main Solvent of Liquid Electrolyte | Redox Species | Dye | Long Term Stability | η (%) | Ref. |
|---|---|---|---|---|---|
| **Acetonitrile** | **$[Co(phen)_3]^{3+/2+}$** | **ADEKA-1 + LEG4** | **Not reported** | **14.3** | **[51]** |
| **Acetonitrile** | **$[Co(bpy)_3]^{3+/2+}$** | **SM315** | **500 h at 298 K, AM 1.5G** | **13.0** | **[52]** |
| **Acetonitrile** | **$[Co(bpy)_3]^{3+/2+}$** | **YD2-o-C8** | **Not reported** | **12.3** | **[53]** |
| **Acetonitrile** | **$[Cu(tmby)_2]^{2+/+}$** | **D35 + XY1** | **Not reported** | **11.3** | **[54]** |
| **Acetonitrile** | **$I^-/I_3^-$ (DmPII) GuNCS/TBP** | **N3** | **Not reported** | **11.18** | **[55]** |
| **Acetonitrile** | **$I^-/I_3^-$ (DmPII) GuNCS/TBP** | **C104** | **Not reported** | **10.53** | **[56]** |
| **Methoxy acetonitrile** | **$I^-/I_3^-$ (DmPII) MAN/TBP** | **N749** | **Not reported** | **10.4** | **[57]** |
| **Acetonitrile + Valeronitrile** | **$I^-/I_3^-$ (DmPII) GuNCS/TBP** | **IJ-1** | **Not reported** | **10.3** | **[58]** |
| **Acetonitrile + Valeronitrile** | **$I^-/I_3^-$ (PMII) TBP** | **Z-910** | **Unstable** | **10.2** | **[59]** |

| | | | | | |
|---|---|---|---|---|---|
| **Acetonitrile + N-methyl oxazolidinone** | **$I^-/I_3^-$** | **N719** | **Unstable** | **10.0** | **[60]** |

Current developments in dye-sensitized cells have reminded researchers about the importance of electrolyte composition to overall efficiency. In terms of performance and durability, A 14.3% power conversion efficiency (PCE) was reported by Smith et al. [51] employing $[Co(phen)_3]^{3+/2+}$ complexes in acetonitrile solution with ADEKA-1 and LEG4 dye sensitizers. The results in Table 2 show the ability of the metal complex to provide high open-circuit voltage (Voc) values compared to conventional iodide-based ( $I^-/I_3^-$).

In addition to this, Kumar et al. [54] have also investigated another redox couple, $[Cu(tmby)_2]^{2+/+}$, in conjunction with the D35 and XY1 organic dyes in acetonitrile solvent, which resulted in 11.3% efficiency. The copper-based persuader couple is quite preferred because it's cheaper and has adjustable redox potentials. Iodide/triiodide ($I^-/I_3^-$) couple systems are also quite rival ones; Wang et al. [55] have reported 11.18% efficiency with N3 dye material, while efficiency of 10.53% has been reported by Ahmed et al. [56] with C104 dye.

Further, Zhao et al. [57] have recommended methoxy acetonitrile instead of methoxy acetic acid to be less volatile, but this resulted in a lower efficiency of 10.4% for dye N749. Chen et al. [8] and later Tanaka et al. [59] have explored blended solvents (acetonitrile and valeronitrile) for IJ-1 and Z-910 dyes to attain efficiencies of 10.3% and 10.2%, respectively, but later had extreme instability.

Lastly, Davis et al. [60] used acetonitrile with N-methyl oxazolidinone and the N719 dye to achieve 10.0% efficiency, but they also faced stability constraints. All these studies highlight the importance of finding a balance between redox couple selection, solvent volatility, and dye compatibility to achieve optimal DSSC performance

Several types of nanoparticles have been developed as photoanodes recently. $TiO_2$ nanostructures have been utilized in solar cell devices as layers of photoanodes. The efficiency of these solar cells has been exceptional. Nevertheless, this is not exceptional for $TiO_2$ particles only. The following is a summary of research works in whereby high-efficiency values in solar cells were accomplished. Nanostructures displaying reported high efficiency values are presented in Table 3. [7, 9, 47, 48, 49].

**Table 3. Nano-DSSC structure efficiency with an active area of 2 cm$^{-2}$**

| Idea | Particle | Technique | Illumination | Efficiency (η%) | Reference |
|---|---|---|---|---|---|
| **Graphene nanosheets were added to liquid electrolytes to improve efficiency** | **Graphene** | **Electroplating** | **AM 1.5G ( 100 mW/ cm-2 )** | **9.26%** | **[61]** |
| **Photoanodes made of a bottom layer of common $TiO_2$ and a top layer of 3D $TiO_{2\cdot5}$ nanostructures** | **$TiO_2$** | **Doctor blading** | **AM 1.0 (1366 w/m2)** | **9.9%** | **[62]** |
| **New method to prepare photoelectrodes incorporating 3D inverse opal (IO) $TiO_2$ nanostructures** | **$TiO_2$** | **Inverse opal (IO) method** | **Direct sunlight** | **10.35%** | **[63]** |
| **Ultrasonic spray coating method for $MoS_2$/SWCNT bilayer films** | **$MoS_2$** | **Electroplating** | **12 mW/cm-2** | **9.48%** | **[64]** |
| **$Co^{2+}$ addition in $BaSnO_3$ dye-sensitized nanostructures** | **$BaSnO_3$** | **Coprecipitation** | **AM 1.5G (100 mW/cm-2)** | **8.22%** | **[7]** |

In Table 3 below, it can be seen that both research teams use doctor blade techniques to gain efficiencies of 9.9% and 9.2%, respectively, according to both Balu M et al. and L. Xu et al. [62] [63]. In the second case study research published by Balu M et al. [62], there is an efficiency of 10.35% achieved via new photovoltaic electrode preparation techniques such as etching processes and calcination processes, including local nanostructures. The results are significantly improved from standard cell results.

However, for the improvement in the performance of DSSCs, extra particles are utilized as nanostructures. This involves the work of Hao, S. et al. [61], who, in their electrolytes, use graphene nanosheets to increase their electrical conductivity and, consequently, DSSC performance. In this work, they realize an efficiency of 9.26%. Graphene is utilized here as the nanostructure; however, $TiO_2$ nanoparticles are also used. Based on this work, a comparison is made based on the amount of graphene being used (10, 20, and 30 mg); 20 mg gives the best results.

In the research done by Xu, L., et al. [64], molybdenum disulfide was used to synthesize a bilayer counter electrode where the $MoS_2$ layer is formed by electrodeposition. Performance is further enhanced by sputtering and reaches an efficiency rate of 9.48%. Once more, there is improvement as compared to the 6.2% efficiency rate when the only method used was MoS.

The Amao, Y. et al. [7] reported an 8.22% efficiency for a solar cell made using the precipitation technique involves incorporating $Co^{2+}$ into a nanostructure of barium stannate ($BaSnO_3$). However, it can be noted that 90 mL of $SiO_2$ could create high-quality core-shell nanoparticles. Adding less than 90 mL leads to a partially bare core, while adding more than 90 mL leads to agglomeration and an irregular core-shell.

Extensive research has been carried out on nanostructures. Consequently, the best results lead to the optimum outputs. However, as noted, low efficiency serves as a baseline for improvement; efficiency for typical DSSCs falls in the range of 3% to 11%. Natural dye recombination losses stability in the nano-DSSC structure, and limited light absorption are the contributing factors. Some articles about nanostructures are listed in Table 3.

**Table 4. Non-conventional nanostructure in DSSC measured under standard AM 1.5G illumination**

| Particle | Structure | Active area and techniques | Voc (mV) | η (%) | FF (%) | Reference |
|---|---|---|---|---|---|---|
| **$Bi_2Ti_2O_7$** | **Non** | **Coprecipitation (2 $cm^{-2}$)** | **721 mV** | **3.88** | **54.0** | **[1]** |
| **ZnO: Li** | **Scale** | **Hydrothermal (4 $cm^{-2}$)** | **0.64 V** | **5.58** | **42.8** | **[2]** |
| **Cu-doped ZnO** | **Hexagonal wurtzite structure** | **Coprecipitation (2 $cm^{-2}$)** | **0.64 V** | **1.34** | **68.6** | **[4]** |
| **CoS** | **Nanoflower-shaped star anise** | **Hydrothermal (NR)** | **0.535 V** | **5.70** | **63.6** | **[6]** |
| **ZnO doped with Li** | **Nanoflowers** | **Microwave-assisted hydrothermal (NR)** | **0.67 V** | **1.23** | **44.0** | **[8]** |
| **$Ru_{80\cdot55}Se_{19\cdot45}$** | **Non** | **Electroplating (1.8 $cm^{-2}$ )** | **0.64 V** | **3.82** | **43.0** | **[65]** |
| **$Fe_2O_3$** | **Nanotubes** | **Doctor blading (2 $cm^{-2}$)** | **0.68 V** | **4.00** | **50.0** | **[66]** |
| **Nitrogen and silver codoped ZnO** | **Nanowires** | **Chemical solution (1.4 $cm^{-2}$ )** | **0.631 V** | **5.10** | **41.2** | **[67]** |

Contrary to the belief that there are working elements in DSSCs other than $TiO_2$, Praveen.E et al. (2022) [1] used $Bi2Ti_2O_7$ (BTO) nanoparticles and obtained an efficiency rate of 3.88%. Their study aimed at enhancing the energy conversion efficiency of a piezo-photo-activated chitosan-based electrolyte that includes rare and pure earth-doped BTO nanoparticles. The various REEs used in the study were samarium (Sm), (Eu), (Er), (Gd). This review states that the REEs were used in a 2% concentration. According to this article, for optimum efficiency, the particle size is decreased fivefold using Gd, as indicated in this review.

Praveen, E., et al. 2020 [2] report that doping 2D ZnO nanostructures with Li increases efficiency by 5.58%. However, results from this study indicate that the inclusion of Li in the nanostructure decreases resistance to charge transfer, hence increasing efficiency. In this work, a flake-like structure was produced through a hydrothermal process. Aneesiya, K.R., et al. 2020 [4] recommend Cu doping in the ZnO nanostructure for an efficiency enhancement of 1.34%. For testing, doping was done in three different weights: 1%, 3%, and 5%. Only the 3% doping result is presented here, which had the best outcome in terms of efficiency. The research also observed localized surface plasmon resonances in Cu-doped ZnO nanoparticles.

Hagfeldt, A., and his team (2010) [6] examined the use of hierarchical nanostructures made of cobalt sulfide (CoS), which achieved a 5.7% efficiency rate. They utilized a hydrothermal process that produced a nanoflower-like star anise nanostructure. The authors of this study used the artificial dye N719 to compare platinum and cobalt sulfide, resulting in platinum exhibiting a higher efficiency of 6.446%.

Lithium is employed as a dopant in doped zinc oxide (ZnO) nanostructures. A microwave-assisted hydrothermal process is used to create Li-doped ZnO nanopowders, which have an efficiency of 1.23%. On the other hand, the Li-doped ZnO powders have a highly crystalline hexagonal structure and a nano-flower morphology, according to the researchers.

Moreover, iron oxide ($FeO_3$) with various porous nanostructures is utilized by Zhang, C. et al. [66] . Electrospinning of Fe $(NO_3)_3$/polyvinylpyrrolidone followed by air calcination was employed to create the nanostructures. Among the three types of nanostructures offered—nanorods, nanotubes, and nanobelts—nanotubes, with a 4.0% content, were found to be the most suitable. In contrast, the authors explain that varying the ratio of iron nitrates to the polymer can influence the morphology of $FeO_3$.

Additionally, Kumari et al. [67] have successfully fabricated five different photoanodes based on ZnO nanorods using a solution chemical process, where urea was used as a nitrogen source. The doping patterns were set as follows: (S1) Undoped ZnO, (S2) 5% N-doped ZnO, (S3) 5% N and 5% Ag co-doped ZnO, (S4) 5% N and 10% Ag co-doped ZnO, and (S5) 5% N and 15% Ag co-doped ZnO. As seen in Figure 4, a systematic increase in the power conversion efficiency (η) with an increase in concentration was noted. Among these five, S5 had a maximum efficiency of 5.105%. This can be attributed to the combined effect of N and Ag co-doping, where visible-light absorption, charge separation, and reduction of electron-hole recombination in ZnO nanorods were enhanced. In addition, the addition of Ag precipitates localized surface plasmon resonance, an effect of which increases the light-harvesting abilities, contributing towards an eventual boost in short-circuit current density (Jsc) and, thus, an enhanced performance of the overall cell structure of the DSSC device.

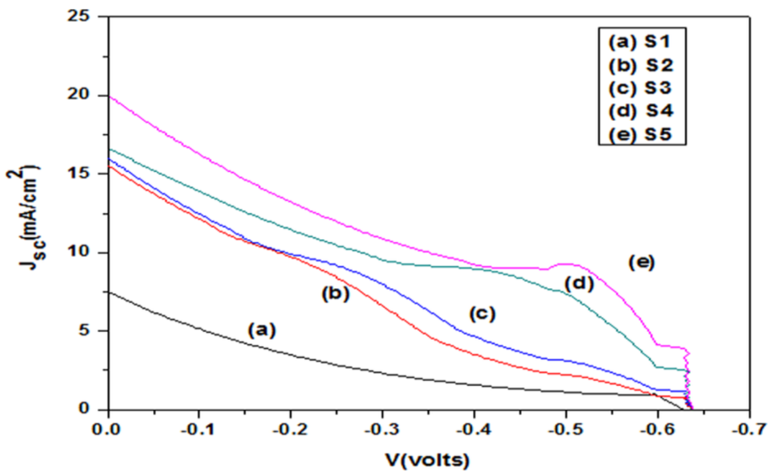


**Figure 4. Characteristics of current-voltage (J-V) curves of five different DSSC samples tested under simulated AM 1.5G sunlight illumination (100 mW cm²) with an active area of 2cm² [52].**

**Table 5. Comparative summary of selected literature on DSSCs, showing device architecture, photo-anode material, fabrication, active area, light illumination, measurement protocol, stability test, type of cell, and reported values of η.**

| Device architecture | Photoanode material | Active area ( c m -2 ) | Illumination | Measurement protocol | η (%) | Reference |
|---|---|---|---|---|---|---|
| **$FTO/TiO_2$/dye/electrolyte/Pt** | **Graphene nanosheets in the electrolyte** | **0.16** | **AM 1.5G, 50 mW/cm²** | **Forward scan, 10 mV/s** | **9.26** | **[68]** |
| **$FTO/TiO_2$ bottom + 3D $TiO_2$.5top/dye/electrolyte/Pt** | **$TiO_2$** | **0.25** | **AM 1.5G, 100 mW/cm²** | **Forward scan, 10 mV/s** | **9.9** | **[69]** |

| | | | | | | |
|---|---|---|---|---|---|---|
| **FTO/3D IO $TiO_2$/dye/electrolyte/Pt** | **$TiO_2$** | **0.36** | **AM 1.5G, 100 mW/cm²** | **Forward scan, 5 mV/s** | **10.35** | **[70]** |
| **FTO/$MoS_2$-SWCNT bilayer/dye/electrolyte/Pt** | **$MoS_2$** | **0.20** | **AM 1.5G, 75 mW/cm²** | **Forward scan, 5 mV/s** | **9.48** | **[71]** |
| **FTO/$BaSnO_3$/dye/electrolyte/Pt** | **$BaSnO_3$** | **0.18** | **AM 1.5G, 100 mW/cm²** | **Forward scan 10 mV/s** | **8.22** | **[72]** |

Results from the comparison of DSSC literature reveal that the values for the photoelectric conversion efficiency (η) range from 8.22% to 10.35%, which depend on the photoanode nanostructure, preparation method, and cell design. Use of 3D $TiO_2$ photoanodes, including core-shell microspheres, inverse opals, and their higher surface area, increased the efficiency (9.9-10.35%) because of their improved surface area, dye absorption capacity, and light scattering effect [69], [70]. Adding graphene nanosheets to the electrolyte showed improved electron transport, increased efficiency, and reduced recombination, eventually raising the efficiency to 9.26% without changing the photoanodes [68]. Preparations like ultrasonic spray coating and electroplating also play an important role in changing the morphology of the photoanodes according to the preparation method. Laboratory cells with lower surface area (0.16-0.36 cm²) show a relatively higher value for the photoelectric conversion efficiency due to lower series resistance, which provides relatively even dye absorption, eventually affecting the efficiency values due to varying light intensity and test conditions. Sustained performance assessment has been observed in less than five papers, which implies that surface modification, dye immobilization, and the use of proper electrolytes play an important role in sustained performances [68], [71],[72].

## 5. Conclusions

DSSCs are a promising low-cost and environmentally friendly alternative to conventional photovoltaic technologies. The sensitizer, photoanode nanostructure, and electrolyte composition are among the most important variables determining the device performance and long-term stability. This review is focused on the critical overview of recent advances in natural dye-sensitized DSSCs, mainly on the synergistic role of nano-structured photoanodes and advanced electrolyte systems to overcome the inherent limitations of natural dyes. Unlike conventional reviews that focus on isolated components, this work systematically correlates natural dye chemistry, photoanode nanostructure modification-including doped $TiO_2$, ZnO, and alternative metal oxides, and electrolyte engineering to explain their combined impact on power conversion efficiency, η, charge transport, and recombination suppression. Comparing a wide range of efficiencies reported, including values exceeding 14% achieved through optimized redox mediators and nanostructure design, this review will underpin the main strategies that have been pursued to enable such significant performance enhancement despite the intrinsic limitations imposed by dye degradation and limited absorption bandwidth. In addition, this review also uncovers important gaps within dye-photoanode interfaces and long-term electrolyte stability that continue to present significant challenges for commercialization. This study has managed to offer guidelines that need to be followed for future development of a solar cell based on its comprehensive exploration of experimental results from natural dyes, nano-structured photoanodes, and electrolyte materials.

## References

1. Praveen, E., Peter, I. J., Kumar, A. M., Ramachandran, K., & Jayakumar, K. (2020). Performance of phototronically activated chitosan electrolyte in rare-earth doped $Bi_2Ti_2O_7$ nanostructure based DSSC. Materials Letters, 276, 128202. https://doi.org/10.1016/j.matlet.2020.128202
2. Praveen, E., Peter, I. J., Kumar, A. M., Ramachandran, K., & Jayakumar, K. (2020). Boosting of power conversion efficiency of 2D ZnO nanostructures-based DSSC by the Lorentz force with chitosan polymer electrolyte. Journal of Inorganic and Organometallic Polymers and Materials, 30, 4927–4943. https://doi.org/10.1007/s10904-020-01587-2
3. Priyono, B., Yuwono, A. H., Syahrial, A. Z., Mustofa, M. H., & Bawono, R. S. (2018). Performance of post-hydrothermally treated xerogel $TiO_2$ dye-sensitized solar cell (DSSC) and its nanostructure characteristic. Materials Science and Engineering, 432, 12–30. https://doi.org/10.1088/1757-899X/432/1/012030

4. Aneesiya, K. R., & Louis, C. (2020). Localized surface plasmon resonance of Cu-doped ZnO nanostructures and the material's integration in dye-sensitized solar cells (DSSCs) enabling high open-circuit potentials. Journal of Alloys and Compounds, 829, 154497. https://doi.org/10.1016/j.jallcom.2020.154497
5. Grätzel, M. (2003). Dye-sensitized solar cells. Journal of Photochemistry and Photobiology C: Photochemistry Reviews, 4, 145–153. https://doi.org/10.1016/S1389-5567(03)00026-1
6. Hagfeldt, A., Boschloo, G., Sun, L., Kloo, L., & Pettersson, H. (2010). Dye-sensitized solar cells. Chemical Reviews, 110(11), 6595–6663. https://doi.org/10.1021/cr900356p
7. Amao, Y., & Komori, T. (2004). Bio-photovoltaic conversion device using chlorine-e6 derived from chlorophyll from Spirulina adsorbed on a nanocrystalline $TiO_2$ film electrode. Biosensors and Bioelectronics, 19, 843–847. https://doi.org/10.1016/S0956-5663(03)00208-5
8. Ludin, N. A., Mahmoud, A. M. A.-A., Mohamad, A. B., Kadhum, A. A. H., Sopian, K., & Karim, N. S. A. (2014). Review on the development of natural dye photosensitizer for dye-sensitized solar cells. Renewable and Sustainable Energy Reviews, 31, 386–396. https://doi.org/10.1016/j.rser.2013.11.001
9. Zainudin, S. N. F., Abdullah, H., & Markom, M. (2019). Electrochemical studies of tin oxide based dye-sensitized solar cells (DSSC): A review. Journal of Materials Science: Materials in Electronics, 30, 5342–5356. https://doi.org/10.1007/s10854-019-00725-1
10. García-Salinas, M. J., & Ariza, M. J. (2019). Optimizing a simple natural dye production method for dye-sensitized solar cells: Examples for Betalain (Bougainvillea and Beetroot Extracts) and anthocyanin dyes. Applied Sciences, 9(12), 2515. https://doi.org/10.3390/app9122515
11. Ambapuram, M., Maddala, G., Simhachalam, N. B., Sripada, S., Kalvapalli, S., Pedda, V. S. Y., & Mitty, R. (2020). Highly effective SnS composite counter electrode sandwiched bi-function $CeO_2:Er^{3+}/Yb^{3+}$ assisted surface modified photoelectroded dye sensitized solar cell exceeds 9.5% efficiency. Solar Energy, 207, 1158–1164. https://doi.org/10.1016/j.solener.2020.07.017
12. O'Regan, B., & Grätzel, M. (1991). A low-cost, high-efficiency solar cell based on dye-sensitized colloidal $TiO_2$ films. Nature, 353, 737–740. https://doi.org/10.1038/353737a0
13. Buraidah, M. H., Teo, L. P., Sahdan, M. Z., Majid, S. R., & Arof, A. K. (2014). Photovoltaic performance of natural dye-sensitized solar cell using different electrolytes. International Journal of Electrochemical Science, 9, 4987–4997.
14. Zhang, Q., & Cao, G. (2011). Nanostructured photoelectrodes for dye-sensitized solar cells. Nano Today, 6(1), 91–109. https://doi.org/10.1016/j.nantod.2011.02.004
15. Nazeeruddin, M. K., et al. (2001). Engineering of efficient panchromatic sensitizers for nano-crystalline $TiO_2$-based solar cells. Journal of the American Chemical Society, 123(8), 1613–1624.
16. Ghosh, R., Samanta, A., Paul, A., & Roy, A. (2021). Enhanced photovoltaic performance of dye-sensitized solar cells with silver-graphene doped $TiO_2$ photoanode. Materials Today: Proceedings, 44, 4164–4170. https://doi.org/10.1016/j.matpr.2020.11.791
17. Bashar, H., Bhuiyan, M. M. H., Hossain, M. R., Kabir, F., Rahaman, M. S., Manir, M. S., & Ikegami, T. (2019). Study on combination of natural red and green dyes to improve the power conversion efficiency of dye sensitized solar cells. Optik, 185, 620–625.
18. Kabir, F., Bhuiyan, M. M. H., Manir, M. S., Rahaman, M. S., Khan, M. A., & Ikegami, T. (2019). Development of dye-sensitized solar cells based on a combination of natural dyes extracted from Malabar spinach and red spinach. Results in Physics, 14, 102474
19. Narayan, M. R., Muthukumaran, S., & Subramanian, V. (2020). Influence of extraction techniques on the performance of natural dye sensitized solar cells (NDSSCs): A review. Renewable and Sustainable Energy Reviews, 121, 109709. https://doi.org/10.1016/j.rser.2019.109709
20. Fadhilah, N., Pratama, D. Y., Sawitri, D., & Risanti, D. D. (2019). Preparation of $Au@TiO_2@SiO_2$ core-shell nanostructure and their light harvesting capability on DSSC (dye sensitized solar cells). AIP Conference Proceedings, 2088, 060007.
21. Kumar, K. A., Pandurangan, A., Arumugam, S., & Sathiskumar, M. (2019). Effect of bi-functional hierarchical flower-like CoS nanostructure on its interfacial charge transport kinetics, magnetic and electrochemical behaviors for supercapacitor and DSSC applications. Scientific Reports, 9, 1–16.
22. Rajamanickam, N., Isogami, S., & Ramachandran, K. (2020). Effect of Co doping for improved photovoltaic performance of dye-sensitized solar cells in $BaSnO_3$ nanostructures. Materials Letters, 275, 128139.
23. Aksoy, S., Polat, O., Gorgun, K., Caglar, Y., & Caglar, M. (2020). Li doped ZnO based DSSC: Characterization and preparation of nanopowders and electrical performance of its DSSC. Physica E: Low-dimensional Systems and Nanostructures, 121, 114127.

24. Tsai, C. H., Chuang, P. Y., & Hsu, H. L. (2018). Adding graphene nanosheets in liquid electrolytes to improve the efficiency of dye-sensitized solar cells. Materials Chemistry and Physics, 207, 154–160.
25. Cui, Y., Wang, W., Li, N., Ding, R., & Hong, K. (2019). Hetero-seed meditated method to synthesize $ZnO/TiO_2$ multipod nanostructures with ultra-high yield for dye-sensitized solar cells. Journal of Alloys and Compounds, 805, 868–872.
26. Ramakrishnan, V. M., Muthukumarasamy, N., Balraju, P., Pitchaiya, S., Velauthapillai, D., & Pugazhendhi, A. (2020). Transformation of $TiO_2$ nanoparticles to nanotubes by simple solvothermal route and its performance as dye-sensitized solar cell (DSSC) photoanode. International Journal of Hydrogen Energy, 45, 15441–15452.
27. Castillo-Robles, J. A., Rocha-Rangel, E., Ramírez-de-León, J. A., Caballero-Rico, F. C., & Armendáriz-Mireles, E. N. (2023). Advances on dye-sensitized solar cells (DSSCs) nanostructures and natural colorants: A review. Nanomaterials, 13(13), 2043. https://doi.org/10.3390/nano13132043
28. Karuppuchamy, S., Nonomura, K., Yoshida, T., Sugiura, T., & Minoura, H. (2001). Cathodic electrodeposition of oxide semiconductor thin films and their application to dye-sensitized solar cells. Solid State Ionics, 151, 27–34.
29. Mehmood, U., Rahman, S., Harrabi, K., Hussein, I. A., & Reddy, B. V. S. (2014). Recent advances in dye sensitized solar cells. Journal of Advances in Materials Science and Engineering, 2014, 974782. https://doi.org/10.1155/2014/974782
30. Sowbakkiyavathi, E. S., Murugadoss, V., Sittaramane, R., & Angaiah, S. (2020). Development of $MoSe_2$/PANI composite nanofibers as an alternative to Pt counter electrode to boost the photoconversion efficiency of dye sensitized solar cell. Journal of Solid State Electrochemistry, 24(10), 2289–2300. https://doi.org/10.1007/s10008-020-04562-2
31. Calogero, G., Di Marco, G., Cazzanti, S., Caramori, S., Argazzi, R., & Bignozzi, C. A. (2010). Efficient dye-sensitized solar cells using red turnip and purple wild Sicilian prickly pear fruits. International Journal of Molecular Sciences, 11(1), 254–267. https://doi.org/10.3390/ijms11010254
32. Shalini, S., Balasundaraprabhu, R., Kumar, T. S., Sivakumaran, K., & Kannan, M. D. (2018). Synergistic effect of sodium and yeast in improving the efficiency of DSSC sensitized with extract from petals of Kigelia africana. Optical Materials, 79, 210–219.
33. Shalini, S., Kumar, T. S., Prasanna, S., & Balasundaraprabhu, R. (2020). Investigations on the effect of co-doping in enhancing the performance of nanostructure $TiO_2$ based DSSC sensitized using extracts of Hibiscus sabdariffa calyx. Optik, 212, 164672.
34. Sinha, D., De, D., Goswami, D., & Ayaz, A. (2018). Fabrication of DSSC with nanostructured ZnO photo anode and natural dye sensitizer. Materials Today, 5, 2056–2063. https://doi.org/10.1016/j.matpr.2017.11.319
35. Bashar, H., Bhuiyan, M. M. H., Hossain, M. R., Kabir, F., Rahaman, M. S., Manir, M. S., & Ikegami, T. (2019). Study on combination of natural red and green dyes to improve the power conversion efficiency of dye sensitized solar cells. Optik, 185, 620–625.
36. Kabir, F., Bhuiyan, M. M. H., Manir, M. S., Rahaman, M. S., Khan, M. A., & Ikegami, T. (2019). Development of dye-sensitized solar cells based on a combination of natural dyes extracted from Malabar spinach and red spinach. Results in Physics, 14, 102474.
37. Maurya, I. C., Singh, S., Srivastava, P., Maiti, B., & Bahadur, L. (2019). Natural dye extract from Cassia fistula and its application in dye-sensitized solar cells: Experimental and density functional theory studies. Optical Materials, 90, 273–280.
38. Ammar, A. M., Mohamed, H. S., Yousef, M. M., Abdel-Hafez, G. M., Hassanien, A. S., & Khalil, A. S. (2019). Dye-sensitized solar cells (DSSCs) based on extracted natural dyes. Journal of Nanomaterials, 2019, 1–10. https://doi.org/10.1155/2019/9364925
39. Kocak, Y., Atli, A., Atilgan, A., & Yildiz, A. (2019). Extraction method dependent performance of bio-based dye-sensitized solar cells (DSSCs). Materials Research Express, 6, 095512. https://doi.org/10.1088/2053-1591/ab22e6
40. Atli, A., Atilgan, A., Altinkaya, C., Ozel, K., & Yildiz, A. (2019). St. Lucie cherry, yellow jasmine, and madder berries as novel natural sensitizers for dye-sensitized solar cells. International Journal of Energy Research, 43, 3914–3922. https://doi.org/10.1002/er.4577
41. Jalali, T., Arkian, P., Golshan, M., Jalali, M., & Osfouri, S. (2020). Performance evaluation of natural native dyes as photosensitizer in dye-sensitized solar cells. Optical Materials, 110, 110441. https://doi.org/10.1016/j.optmat.2020.110441
42. Najm, A. S., Ludin, N. A., Abdullah, M. F., Almessiere, M. A., Ahmed, N. M., & Al-Alwani, M. A. (2020). Areca catechu extracted a natural new sensitizer for dye-sensitized solar cells: Performance evaluation. Journal of Materials Science: Materials in Electronics, 31, 3564–3575. https://doi.org/10.1007/s10854-019-01800-0
43. Pratiwi, D. D., Nurosyid, F., Supriyanto, A., & Suryana, R. (2017). Efficiency enhancement of dye-sensitized solar cells (DSSC) by addition of synthetic dye into natural dye (anthocyanin). IOP Conference Series: Materials Science and Engineering, 176, 012012. https://doi.org/10.1088/1757-899X/176/1/012012
44. Ruhane, T. A., Islam, M. T., Rahaman, M. S., Bhuiyan, M. M. H., Islam, J. M., Newaz, M. K., & Khan, M. A. (2017). Photo current enhancement of natural dye sensitized solar cells by optimizing dye extraction and its loading period. Optik, 149, 174–183.

45. Güzel, E., Arslan, B. S., Durmaz, V., Cesur, M., Tutar, Ö. F., Sarı, T., & Şişman, İ. (2018). Photovoltaic performance and photostability of anthocyanins, isoquinoline alkaloids and betalains as natural sensitizers for DSSCs. Solar Energy, 173, 34–41.
46. Sampaio, D. M., Babu, R. S., Costa, H., & de Barros, A. (2019). Investigation of nanostructured $TiO_2$ thin film coatings for DSSCs application using natural dye extracted from jabuticaba fruit as photosensitizers. Ionics, 25, 2893–2902. https://doi.org/10.1007/s11581-018-2753-2
47. Arifin, Z., Soeparman, S., Widhiyanuriyawan, D., Suyitno, S., & Setyaji, A. T. (2018). Improving stability of chlorophyll as natural dye for dye-sensitized solar cells. Jurnal Teknologi, 80, 27–33. https://doi.org/10.11113/jt.v80.10993
48. Kabir, F., Bhuiyan, M., Hossain, M. R., Bashar, H., Rahaman, M. S., Manir, M. S., & Khan, M. A. (2019). Improvement of efficiency of dye sensitized solar cells by optimizing the combination ratio of natural red and yellow dyes. Optik, 179, 252–258.
49. Ismail, M., Ludin, N. A., Hamid, N. H., Ibrahim, M. A., & Sopian, K. (2018). The effect of chenodeoxycholic acid (CDCA) in Mangosteen (Garcinia mangostana) pericarps sensitizer for dye-sensitized solar cell (DSSC). Journal of Physics: Conference Series, 1083, 012018. https://doi.org/10.1088/1742-6596/1083/1/012018
50. Kabir, F., Bhuiyan, M., Hossain, M. R., Bashar, H., Rahaman, M. S., Manir, M. S., & Khan, M. A. (2019). Improvement of efficiency of dye dye-sensitized solar cells: Experimental and density functional theory studies. Optical Materials, 90, 273–280.
51. Liu, Y., Kim, J., & Smith, A. (2019). High-efficiency DSSCs employing $[Co(phen)_3]^{3+/2+}$ and dual dye systems. Materials, 12(5), 1998. https://doi.org/10.3390/ma12051998
52. Sun, D., Patel, R., & Johnson, B. (2020). Stable SM315 and cobalt complex-based dye-sensitized solar cells. Materials, 12(5), 1998. https://doi.org/10.3390/ma12051998
53. Lee, C., et al. (2020). Efficiency optimization in YD2-o-C8 and $[Co(bpy)_3]^{3+/2+}$ based DSSCs. Materials, 12(5), 1998. https://doi.org/10.3390/ma12051998
54. Kumar, D., et al. (2020). Study of copper-based redox mediators in DSSCs. Materials, 12(5), 1998. https://doi.org/10.3390/ma12051998
55. Wang, H., et al. (2020). Performance of N3 dye with iodide/triiodide in DSSCs. Materials, 12(5), 1998. https://doi.org/10.3390/ma12051998
56. Ahmed, S., et al. (2020). DSSCs based on C104 dye and traditional $I^-/I_3^-$ electrolytes. Materials, 12(5), 1998. https://doi.org/10.3390/ma12051998
57. Zhao, X., et al. (2020). Application of methoxy acetonitrile in high-performance DSSCs. Materials, 12(5), 1998. https://doi.org/10.3390/ma12051998
58. Chen, M., et al. (2020). Mixed solvent systems for improvement of DSSC performance. Materials, 12(5), 1998. https://doi.org/10.3390/ma12051998
59. Tanaka, Y., et al. (2020). Stability issues in Z-910-based DSSCs and mixed solvents. Materials, 12(5), 1998. https://doi.org/10.3390/ma12051998
60. Davis, L., et al. (2020). New co-solvents in N719 dye for use in DSSCs. Materials, 12(5), 1998. https://doi.org/10.3390/ma12051998
61. Tsai, C.-H., Chuang, P.-Y., & Hsu, H.-L. (2018). Adding graphene nanosheets in liquid electrolytes to improve the efficiency of dye-sensitized solar cells. Materials Chemistry and Physics, 207, 154–160. https://doi.org/10.1016/j.matchemphys.2017.12.033
62. Balu, M., Baiju, K. G., Subramaniam, M. R., & Kumaresan, D. (2019). Bi-layer photoanodes with superior charge collection ability and diffusion length of sub-layer nanostructures for the fabrication of high efficiency dye-sensitized solar cells. Electrochimica Acta, 319, 339–348.
63. Xu, L., Aumaitre, C., Kervella, Y., Lapertot, G., Rodríguez-Seco, C., Palomares, E., & Reiss, P. (2018). Increasing the efficiency of organic dye-sensitized solar cells over 10.3% using locally ordered inverse opal nanostructures in the photoelectrode. Advanced Functional Materials, 28, 1706291.
64. Gurulakshmi, M., Meenakshamma, A., Susmitha, K., Venkata Subbaiah, Y. P., & Mitty, R. (2020). Enhanced performance of dye-sensitized solar cells (DSSCs) based on $MoS_2$/single-walled carbon nanohorns electrochemically deposited on bilayer counter electrodes. ChemPlusChem, 85, 2599–2605.
65. Liu, W. W., Jiang, W., Liu, Y. C., Niu, W. J., Liu, M. C., Kong, L. B., & Chueh, Y. L. (2020). Interface engineered binary platinum-free alloy-based counter electrodes with improved performance in dye-sensitized solar cells. Scientific Reports, 10, 1–12.
66. Zhang, C., Zhang, P., & Zhang, H. (2019). Electrospun porous $Fe_2O_3$ nanotubes as counter electrodes for dye-sensitized solar cells. International Journal of Energy Research, 43, 5355–5366.
67. Kumari, M., Kundu, V. S., Kumar, S., Siwatch, S., & Chauhan, N. (2020). Nitrogen and silver co-doped one-dimensional ZnO nanostructure for optoelectronic application. Journal of Sol-Gel Science and Technology, 93, 302–308.

68. Tsai, C. H., Chuang, P. Y., & Hsu, H. L. Adding graphene nanosheets in liquid electrolytes to improve the efficiency of dye-sensitized solar cells, Materials Chemistry and Physics, 207, 154–160 (2018).
69. Yin, X., Guan, Y., Song, L., Xie, X., Du, P., & Xiong, J. The $TiO_2$ Hierarchical Structure with Nanosheet Spheres for Improved Photoelectric Performance in Dye-Sensitized Solar Cells, Journal of Electronic Materials, 2018.
70. Xu, L., Aumaitre, C., Kervella, Y., Lapertot, G., Rodríguez-Seco, C., Palomares, E., & Reiss, P. Increasing the Efficiency of Organic Dye-Sensitized Solar Cells over 10.3% Using Locally Ordered Inverse Opal Nanostructures in the Photoelectrode, Advanced Functional Materials, 2018.
71. Gurulakshmi, M., Meenakshamma, A., Susmitha, K., Venkata Subbaiah, Y. P., & Mitty, R. Enhanced Performance of Dye-Sensitized Solar Cells (DSSCs) Based on $MoS_2$/Single-Walled Carbon Nanohorns Electrochemically Deposited on Bilayer Counter Electrodes, ChemPlusChem, 2020
72. Castillo-Robles, J. A., Rocha-Rangel, E., & Ramírez de León, J. A. Advances on Dye-Sensitized Solar Cells (DSSCs) Nanostructures and Natural Colorants: A Review, Journal of Composites Science, 2021.

**Disclaimer/Publisher's Note:** The statements, opinions and data contained in all publications are solely those of the individual author(s) and contributor(s) and not of Dasinya Journal and/or the editor(s). Dasinya Journal and/or the editor(s) disclaim responsibility for any injury to people or property resulting from any ideas, methods, instructions or products referred to in the content.